given by[3,4]

$$f = (1/\pi d)(3P_A k/\rho_l)^{1/2} \quad (4)$$

where d is the bubble diameter. For our test conditions, Eq. (4) becomes approximately

$$f = 530/d \quad (5)$$

where d is in inches. Because the bubbles were very small‡ their resonant frequencies were well out of the test frequency range, and they probably contributed very little damping to the system. A more likely explanation for the lower X ratio at resonance is that the damping due to viscous shear and structural relaxation in the water was higher at the lower natural frequency of the mixture. The damping from these sources is[6]

$$\alpha = (\tfrac{4}{3}\eta + \eta')\omega^2/2\rho C^3 \quad (6)$$

where α is the theoretical coefficient of attenuation of acoustic waves, ω is the circular frequency of excitation, ρ and C are the density and sound velocity of the liquid, and η and η' are the shear and volume coefficients of viscosity. Since, in these tests, the frequency ω at which the magnification was measured was directly proportional to C, Eq. (6) can be written for resonant conditions as

$$\alpha \propto (\tfrac{4}{3}\eta + \eta')/\rho C \quad (7)$$

Thus, if the physical constants are approximately the same in the mixture as in the homogeneous fluid, the damping at resonance is inversely proportional to the speed of sound, and higher damping would be expected in the helium-water mixture.

There is some question as to whether the expansion and contraction of the bubbles should be treated analytically as an adiabatic or an isothermal process. Curves for adiabatic theory, Eq. (1), were shown in Figs. 3 and 4a. Figure 4b shows a nondimensional comparison of all frequency data with both adiabatic and isothermal theory, Eq. (2). The adiabatic theory appears to fit the data slightly better than the isothermal theory.

The effect of flow-pipe test section flexibility was not studied experimentally. Calculations based on Eq. (1) indicate that the flexibility of the test section was negligible in these experiments. However, Eq. (1) indicates that in the case of a very flexible pipe (such as might be the case for a launch vehicle propellant line) the speed of sound in the pipe is lowered and the effect of helium on the natural frequencies may be somewhat less than in the rigid pipe case. For example, had the test section wall thickness been 0.025 in. instead of 0.25 in., the first natural frequency would have been 114 Hz instead of 140 Hz. One percent of helium would have lowered this frequency by a factor of 4.7 instead of the factor of 5.6 for the rigid pipe case. Increasing the pipe diameter by a factor of 10 would have a similar effect.

References

[1] Rubin, S., "Longitudinal Instability of Liquid Rockets Due to Propulsion Feedback," *Journal of Spacecraft and Rockets*, Vol. 3, No. 8, Aug. 1966, pp. 1188–1195.

[2] McKenna, K. J., Walker, J. H., and Winje, R. A., "Engine-Airframe Coupling in Liquid Rocket Systems," *Journal of Spacecraft and Rockets*, Vol. 2, No. 2, March–April 1965, pp. 254–256.

[3] Karplus, H. B., "The Velocity of Sound in a Liquid Containing Gas Bubbles," Project A-097, Atomic Energy Commission Contract AF(11-1)-528, June 1958, Armour Research Foundation.

[4] Carstensen, E. L. and Foldy, L. L., "Propagation of Sound Through a Liquid Containing Bubbles," *Journal of the Acoustical Society of America*, Vol. 19, 1947, pp. 481–501.

[5] Laird, D. T. and Kendig, P. M., "Attenuation of Sound in Water Containing Air Bubbles," *Journal of the Acoustical Society of America*, Vol. 24, 1952, pp. 29–32.

[6] Kinsler, L. E. and Frey, A. R., *Fundamentals of Acoustics*, 2nd ed., Wiley, New York, 1962.

‡ Several tests were conducted using two transparent sections in the flow line. Motion pictures at 400 frames/sec showed the helium bubbles to be small and evenly distributed in the water, both at $0g$ and $3.4g$.

Burning Characteristics of Composite Solid Propellants at High Pressures

CHARLES HAFF* AND EUGENE GARNER†
Talley Industries Inc., Mesa, Ariz.

Nomenclature

K_n = area ratio
r_b = burning rate, m/sec
p_c = chamber pressure, psia
C/F = oxidizer granulation ratio, coarse to fine

Introduction

THE usual practice for designing rocket motors for operation at higher pressures is to utilize data obtained from subscale test firings at lower pressures. The data are presented on burning rate (r_b) and K_n plots and are extrapolated to the pressures required for the application. Since most design requirements are at pressures of 3000 psi and lower, experience to date has been satisfactory. Newer applications of propellant systems have dictated that the extrapolations must be reliable to the 5000 to 10,000 psi range. Most propellant systems fail to perform as expected in this region.

This Note describes a series of evaluations performed on "standard" solid propellants and presents some conclusions based on the systems investigated. Burning instability for the purpose of this Note shall be considered as any marked change in K_n slope. The condition of resonant burning or other forms of instability are not considered to be meaningful in the configurations studied.

The propellants chosen for initial evaluation, first six groups in Table 1, are standard formulations and constitute

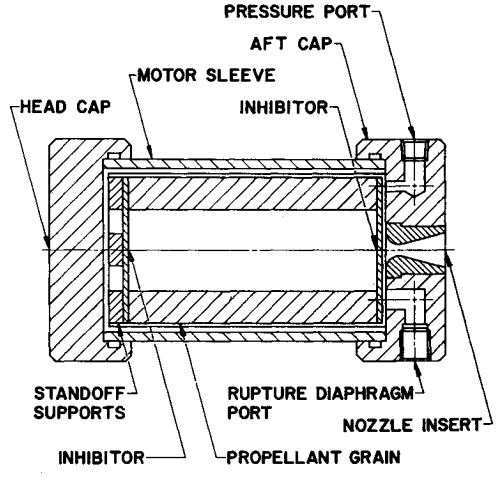

Fig. 1 K_n motor assembly test fixture.

Presented as Paper 69-438 at the AIAA 5th Propulsion Joint Specialist Conference, U. S. Air Force Academy, Colo., June 9–13, 1969; submitted June 4, 1969; revision received July 31, 1969.

* Head, Applied Research Division. Member AIAA.
† Staff Chemist.

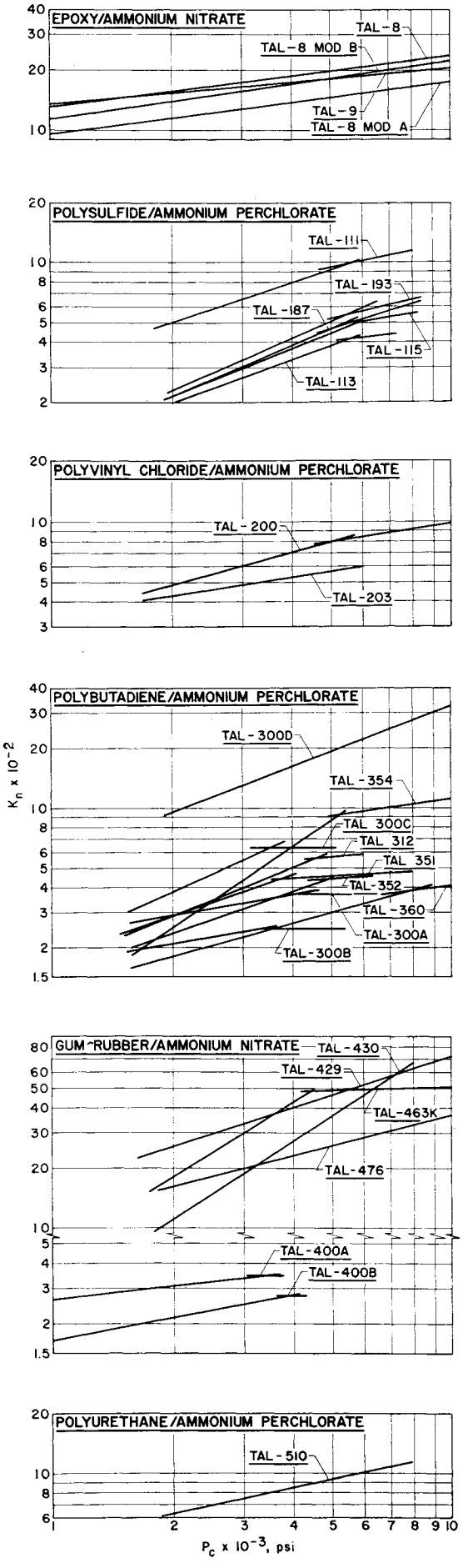

Fig. 2 Pressure and burning time of propellants.

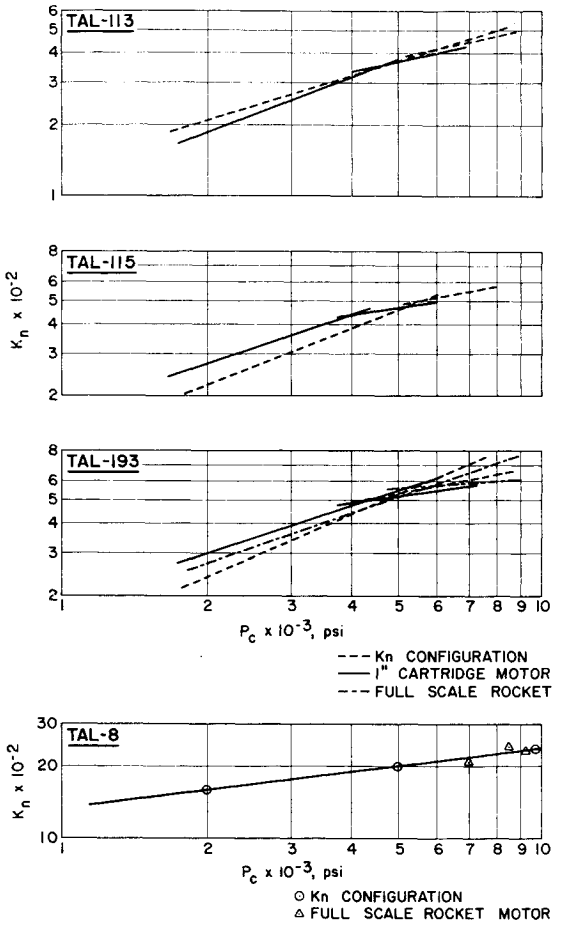

Fig. 3 Effect of rocket motor configuration on critical pressure.

a cross section of normal ingredients. This group also encompasses variations in percentage of these materials within the various formulation classes. In the last four groups in Table 1, propellants were formulated specifically for this program to test a new material and combinations of the standard materials.

The new material utilized in this program was a saturated hydrocarbon binder. Some special combinations produced for this program were gum rubber/ammonium perchlorate, ammonium nitrate/ammonium perchlorate, mixed oxidizers, and unimodal oxidizer particle distributions in standard binders. The variables evaluated are as follows: binder type, oxidizer type, plasticization, burning rate catalyst content, oxidizer particle size distribution, aluminum content, oxidizer loading, solids loading, and mixed oxidizers.

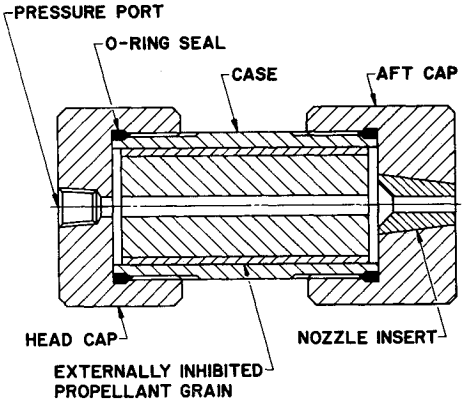

Fig. 4 One inch cartridge motor.

Table 1 Formulation of propellants

GROUP	PROPELLANTS	OXIDIZER LOADING	BINDER	PLASTICIZER	r_b CATALYST	PROCESSING AIDS	C/F RATIO	OXIDIZER BLEND	AMMONIUM NITRATE	AMMONIUM PERCHLORATE	ALUMINUM
1	EPOXY/AMMONIUM NITRATE										
	TAL-8	67.5	24.8	5.0	2.0	0.7	2.33	BIMODAL			
	TAL-9	71.1	22.4	4.0	2.0	0.5	1.00	BIMODAL			
2	GUM RUBBER/AMMONIUM NITRATE										
	TAL-429	82.9	14.3	2.5	0.3						
	TAL-430	77.0	20.4	2.4	0.2			UNIMODAL			
	TAL-463K	77.0	16.3	3.0	3.7						
	TAL-476	80.0	27.2	2.3	1.6						
3	POLYSULFIDE/AMMONIUM PERCHLORATE										
	TAL-111	74.5	20.8	3.2			2.33	BIMODAL			1.6
	TAL-113	78.6	15.9	2.4	1.5		1.40	TETRAMODAL			1.6
	TAL-115	71.8	19.7	3.0	5.5		1.30	TRIMODAL			
	TAL-187	72.4	23.7		1.9		0.88	BIMODAL			2.0
	TAL-193	70.5	24.8		4.7		1.00	BIMODAL			
	TAL-195	70.5	24.8		4.7		1.00	BIMODAL			
	TAL-195A	74.0	21.3		4.7		1.50	BIMODAL			
4	POLYVINYL CHLORIDE/AMMONIUM PERCHLORATE										
	TAL-200	80.0	9.0	11.0			2.33	BIMODAL			
	TAL-203	74.0	11.7	14.3				UNIMODAL			
5	POLYBUTADIENE/AMMONIUM PERCHLORATE										
	TAL-312 (RANDOM POLYMER)	65.6	(14.2)	2.2	1.0		0.55	TRIMODAL			17.0
	TAL-351	78.9	15.5	3.6	2.0		1.02	TRIMODAL			
	TAL-352	79.8	11.0	7.2	2.0		0.80	BIMODAL			
	TAL-354 (DEPRESSANT)	79.8	9.2	6.0	(5.0)		2.40	BIMODAL			
	TAL-360	68.8	8.2	8.0	2.0		2.40	BIMODAL			13.0
6	POLYURETHANE/AMMONIUM PERCHLORATE										
	TAL-510	70.0	15.0	5.0			0.43	BIMODAL			10.0
7	EPOXY/AMMONIUM NITRATE										
	TAL-8 MOD A		26.6	1.4	2.0	1.0	1.00	BIMODAL	49.0	20.0	
	TAL-8 MOD B		22.9	4.0		0.6	1.00	BIMODAL	72.5		
8	BUTYL RUBBER/AMMONIUM PERCHLORATE										
	TAL-300 MOD A	80.0	16.7	3.3				UNIMODAL			
	TAL-300 MOD B	80.0	16.7	3.3			2.33	BIMODAL			
9	POLYBUTADIENE/AMMONIUM PERCHLORATE NITRATE										
	TAL-300 MOD C		11.2	6.0			2.33	BIMODAL	5.0	77.0	
	TAL-300 MOD D		12.7	11.5			2.33	BIMODAL	15.0	60.8	
10	GUM RUBBER/AMMONIUM PERCHLORATE										
	TAL-400 MOD A	80.0	16.7	3.3			2.33	BIMODAL			
	TAL-400 MOD B	80.0	16.7	3.3				UNIMODAL			

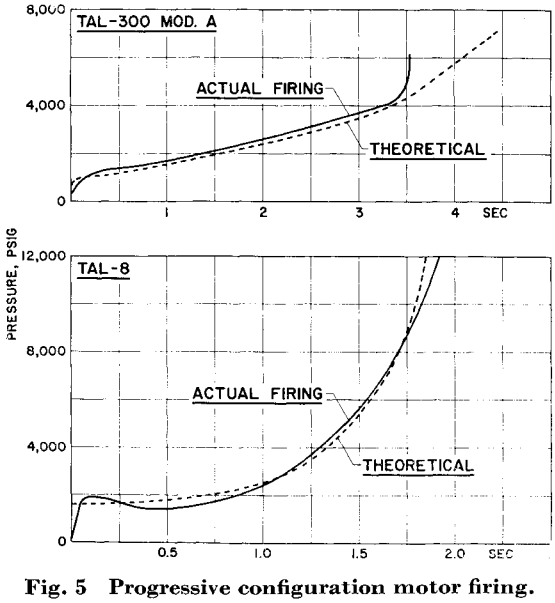

Fig. 5 Progressive configuration motor firing.

Experimental Procedures

Propellant samples were machined to K_n configuration, a 4-in.-long ported cylinder with a 3-in. o.d. and a 1-in. i.d. port. The grains are end-inhibited to produce an internal/external burning grain with constant burning surface. The units are enclosed in a test fixture (see Fig. 1) and fired at ambient temperature. Pressure and burning time are recorded for each firing. Changes in K_n slope are taken as evidence of instability (Figs. 2 and 3). Critical pressures are estimated from the intersections of the K_n slopes.

Cartridge-loaded miniature motors, (Fig. 4) using a single perforated grain, burning internally and at both ends, dimensioned for a relatively neutral pressure vs time trace, and full-scale production motors designed for high operating pressures were also utilized for this program.

One additional configuration was included in the program to evaluate the configuration for its intended purpose as well as to establish propellant stability. This configuration is a progressive-burning grain inhibited on both ends and outside surface, which is designed to exceed the stable pressure limit of the propellant. Use of a computer is required for this procedure. The computer program is designed to extrapolate

a pressure vs time trace based on the known low-pressure data. The grain is fired normally and the pressure vs time trace is reduced for a given number of time increments and the pressures obtained at these increments are used as input to the computer program. The actual pressure vs time trace is replotted by the computer to the same time base as the original theoretical trace. The comparison of the two traces then defines the point of instability if it exists in the pressure region investigated (Fig. 5).

Results

Epoxy/ammonium nitrate propellants exhibited stable burning up to 12,000 psi. Modification of particle size distribution, plasticizer, or replacement of up to 30% of the nitrate with ammonium perchlorate had no effect on the stability limit.

Gum rubber/ammonium nitrate propellants generally demonstrate stable burning up to 10,000 psi. Inclusion of burning rate catalyst content of 4% reduces critical pressure to 4700 psi. Oxidizer loading and plasticizer content had no significant effect. Replacement of the nitrate with ammonium perchlorate resulted in a critical pressure of 3600 psi.

Polysulfide/ammonium perchlorate propellants are stable to the 5000–6000 psi range. Increases of burning rate catalyst and fine oxidizer content tends to decrease stability. Plasticizer or aluminum content, in quantities of two to three percent are not significant to stability.

Polyvinyl chloride/ammonium perchlorate propellants tend to greater stability with lower oxidizer content, in these cases the more stable formulation contains only fine oxidizer.

Polybutadiene/ammonium perchlorate propellants exhibit unstable burning from 3400 to 7000 psi dependent upon formulations. The least stable system contains random-terminated polymer, an intermediate is a saturated hydrocarbon, and the most stable system is the carboxy-terminated polymer. Generally, for the carboxy-terminated polymer, as solids and plasticizer content increase so does the critical pressure. Oxidizer particle size distribution appears to have no effect on the pressure stability of the propellant. Replacement of perchlorate with ammonium nitrate tends to increase the critical pressure.

Crew Locomotion Disturbances in a Space Cabin Simulator

M. Goodman* and W. C. Middleton†
McDonnell Douglas Astronautics Company, Santa Monica, Calif.

Introduction

Over the long run, crew locomotion disturbances to a space vehicle may be essentially cancelled out by return trips between stations in the vehicle. However, appreciable attitude errors can develop prior to this cancellation. Thus, it will be necessary to counteract these disturbances continuously as they occur by means of control torques generated by control moment gyros (CMGs), reaction control thrusters, or combinations of both. In the latter case, the thrusters are used to desaturate the CMG and to provide the simultaneous stationkeeping functions.

The magnitude of disturbance and net impulse imparted per event have been determined for three types of locomotion:

Received June 20, 1969; revision received July 31, 1969.

* Senior Engineer Scientist, Western Division. Associate Fellow AIAA.

† Senior Engineer Scientist, Western Division.

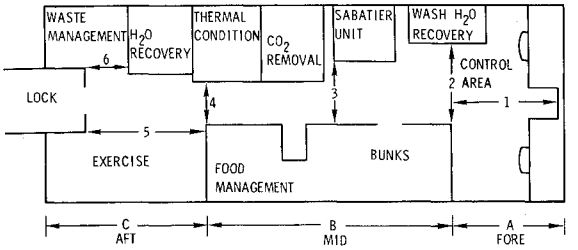

Fig. 1 Location of photoelectric light beams in the SCS.

free soaring, velcro walking, and hand rail walking, while the test subject was suspended to simulate the zero-gravity environment of a space vehicle.[1] However, little information has been available for predicting the frequency of locomotion to be expected within a space vehicle. An opportunity to obtain data on crew locomotion became available during an extended test of a life support system in the MDAC Space Cabin Simulator (SCS).[2] This Note presents some data on the locomotion of four crewmen during six separate 24-hr periods of a 60-day continuous test in the SCS. Six photoelectric relays and their associated light sources were installed within the SCS for this purpose (see numbers 1–6 and their light paths in Fig. 1). When a light beam was interrupted, one of six pens in an event recorder was activated. The cylindrical SCS, 12 ft in diameter and 40 ft long, contained the basic components of a life support system and hence simulated the geometry of a typical space station.

Test Results

The results of the crew travel studies were reported with the SCS arbitrarily divided into three general areas: 1) the forward command area, 2) the midgalley area, and 3) the aft waste management and exercise area. The crewmen spent considerably more time in the command area, which was the focal point in the SCS; most crew travel began and terminated in this area. Table 1 shows the round-trip travel between the three areas during each of the six 24-hr periods that were monitored. Travel on Sunday was obviously less than travel during the week days. This was expected because of the greater activity outside of the SCS on week days. There was no significant change in the amount of travel as the run progressed. For example, the same number of round trips were made on Tuesday, February 27, 1968 and on Tuesday, April 9, 42 days later. During the latter part of the 60-day run, there was an increase in the percentage of the day's travel activity that occurred between the command station and the galley, and less activity occurred in the vicinity of the exercise area.

Figure 2 shows the total activity as evidenced by photocell activations recorded within the SCS from 8:00 AM, Sunday, April 7, 1968 to 8:00 AM, Monday. This includes activity within each area and travel between the areas. These data are presented for a Sunday because the crewmen received fewer extraneous inputs from outside of the SCS on this day. The sharp peak in activity at midnight was caused by one crewman who paced back and forth each night as part of his

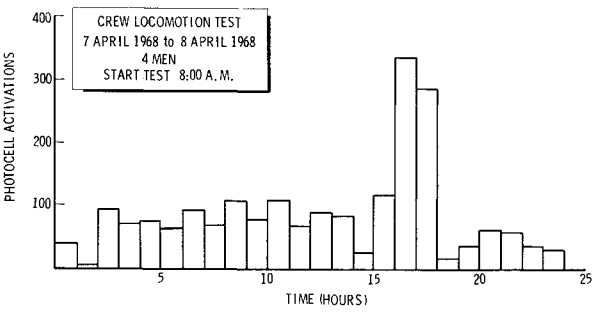

Fig. 2 Photocell activations vs time.